Electronic Supplementary Material (ESI) for Nanoscale Horizons.


# Supplementary Information

## Twisted Light Induced Magnetic Anisotropy Changes in an Interlayer Exchange Coupling System

Chun-I Lu,[1] Shang-An Wang,[1] Kristan Bryan Simbulan,[1] Chak-Ming Liu,[1] Xiao Wang,[2] Guoqiang Yu,[2] Wen-Chin Lin,[1] Ting-Hua Lu*[1] and Yann-Wan Lan*[1]

*[1]Department of Physics, National Taiwan Normal University, Taipei, Taiwan*

*[2]Beijing National Laboratory for Condensed Matter Physics, Institute of Physics, University of Chinese Academy of Sciences, Chinese Academy of Sciences, Beijing, China*

*thlu@ntnu.edu.tw

*ywlan@ntnu.edu.tw

**Magnetic flux in different topological charge values of twisted light**

Figure 1(c) and 1(d) in the main context show the electrical current density and the corresponding perpendicular magnetic field of the $l = 5$ twisted light. Here, Figure S1(a) present the magnetic field established by different topological charge values of twisted light. The x-axis unit, $w_0$, represents the radius of beam in $l = 0$. The magnetic flux of Figure S1(b) is the integration results ($\int_{-\infty}^{\infty} B \cdot dA$) of Figure S1(a). We can summarize that, as the topological charge increasing, the magnetic flux increasing is as expected.

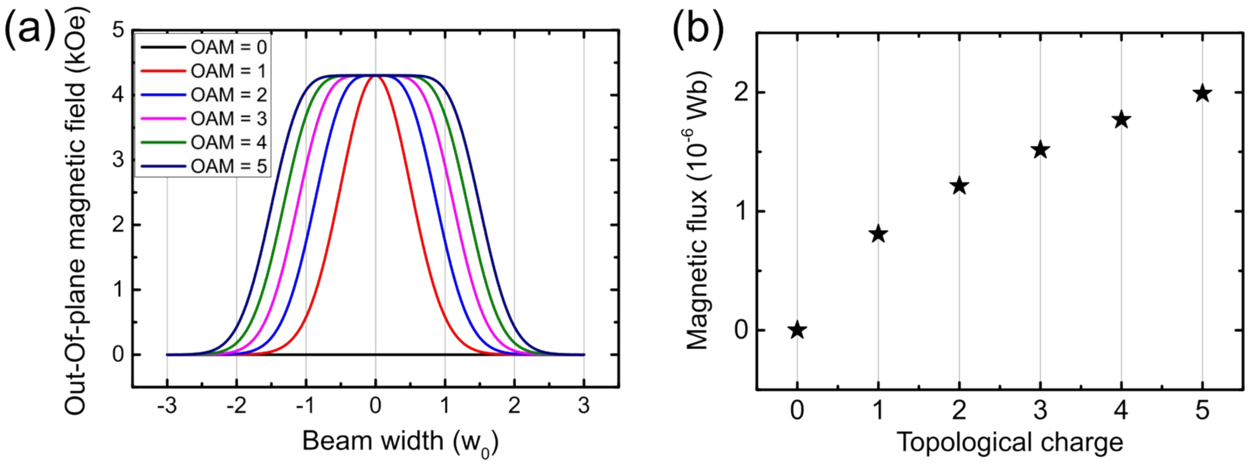


Figure S1 (a) The line profile of the perpendicular magnetic field established by the surface vortex electrical current. The highest magnetic field is the same for all non-zero OAM. As the topological charge increases, the beam width would also increase so that the effective area becomes larger when $l = 5$. (b) The calculated magnetic flux is based on the integrating of Figure S6(a). The magnetic flux is increasing when the topological charge increase.

**Incident power and topological charge versus coercivity of sample**

In the manuscript, Figure 3 shows the comparison of the coercivity of the sample after the different incident twisted light irradiations. Here, Figure S2 shows the collecting data of Figure 3. Figure S2(a) is the chart of the topological charge vs. the sample's coercivity and Figure S2(b) is the chart of the light power of the $l = 5$ twisted laser vs. the sample's coercivity, respectively. The sample's coercivity has a decreasing tendency when the beam's topological charge and power increasing. However, as the hysteresis loops in Figure 3(a) show, the dramatic dropping of coercivity happens at $l = 5$ and incident power at 2.5 mW. Note that, the data points at $l = 0$ and incident power at 0 in Figure S2, are the coercivities of the sample before light illumination in Figure 3(a) to 3(c).

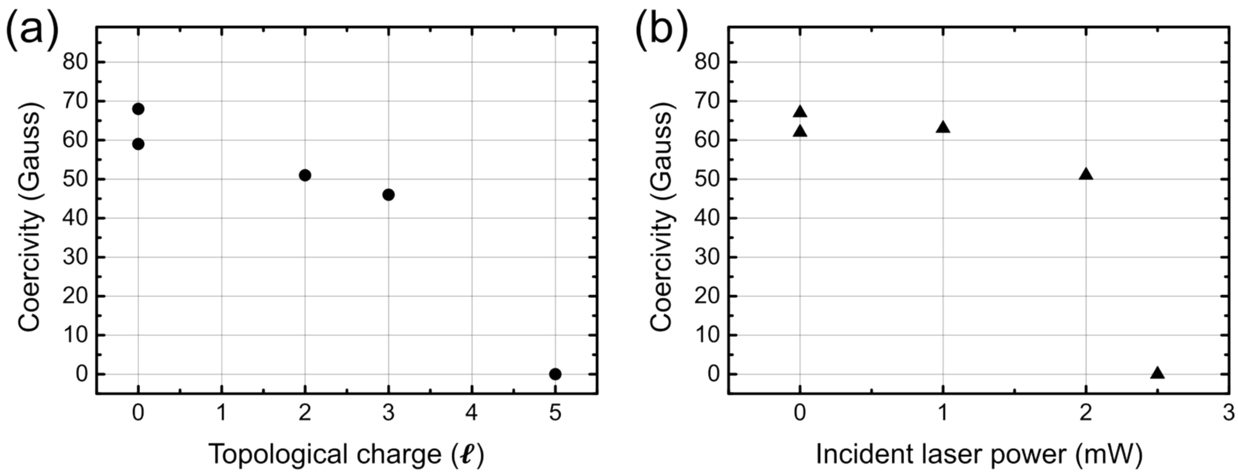


Figure S2 (a) The chart of incident twisted light's topological charge v.s. sample's coercivity after light irradiation. (b) The chart of incident $l = 5$ twisted light's power v.s. sample's coercivity after light irradiation. Both charts were collected from Figure 3.

**The control experiment of no interlayer-exchange coupling**

To verify the role of the interlayer-exchange-coupling plays, which was suggested to provide a pinning effect for stabilized the magnetization. A heterostructure thin-film Pd (5 nm)/ Co (3 nm)/ Pd (5 nm) on a $SiO_2$ substrate was prepared as the control experiments. The comparison of the MA measurements is shown in Figure S1. The identical MA distributions imply although the magnetization could be tuned by the twisted light, IEC effect is another key to stabilize the spin configuration.

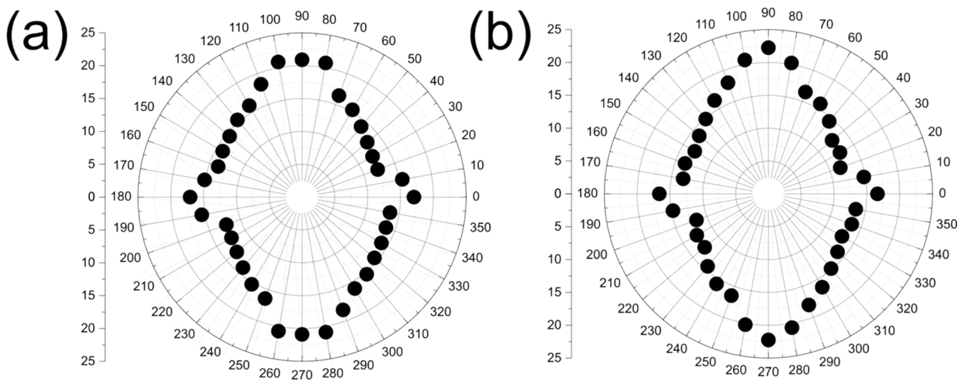


Figure S3. A MA comparison between the cases of (a) before twisted light illumination and (b) after twisted light illumination of the Pd(5 nm)/Co(3 nm)/$SiO_2$ heterojunction.

**The complete data set of the magnetic anisotropy measurement**

In this section, the complete data sets of Figure 4 are provided in Figure S4 and Figure S5 to give readers the details of MA changing. Figure S4 is the data set before twisted light illumination and Figure S5 is the data set after.

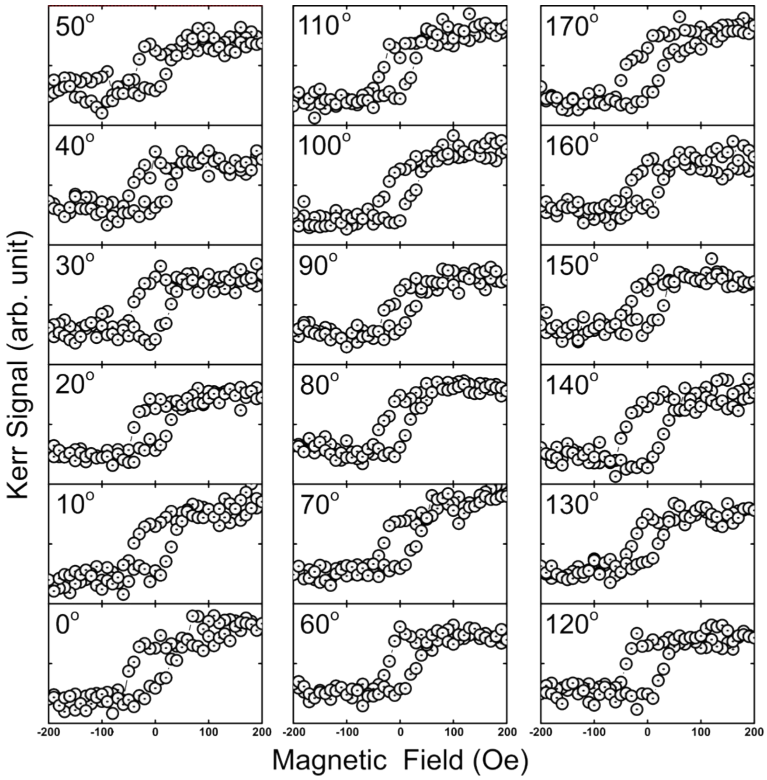


Figure S4. The data set of the hysteresis loops of the sample before twisted light illumination at each angle.

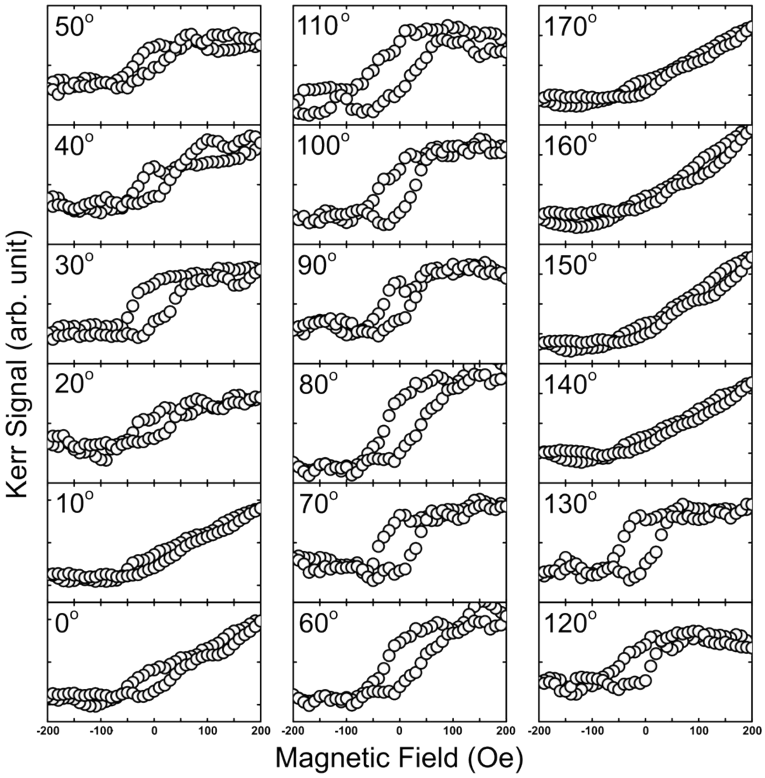


Figure S5. The data set of the hysteresis loops of the sample after twisted light illumination at each angle.

## The effect of MA changing of the negative $l$ and vertical magnetic field on the IEC devices

In this section, we would like to present the negative topological charge $l$ could also modify the sample's MA as well. In Figure S6, the first polar diagram represents the initial MA state of the sample (not yet illuminated with twisted light). And the second polar diagram is the MA state after illuminating with $l = 5$ twisted light. The MA orientation was modified (rotated) as expected. The third polar diagram is the MA state of the same sample in which we illuminated $l = -5$ twisted light immediately after the second MA measurement. The MA orientation concludes firmly that the sample's spin configuration was disturbed again by the twisted light.

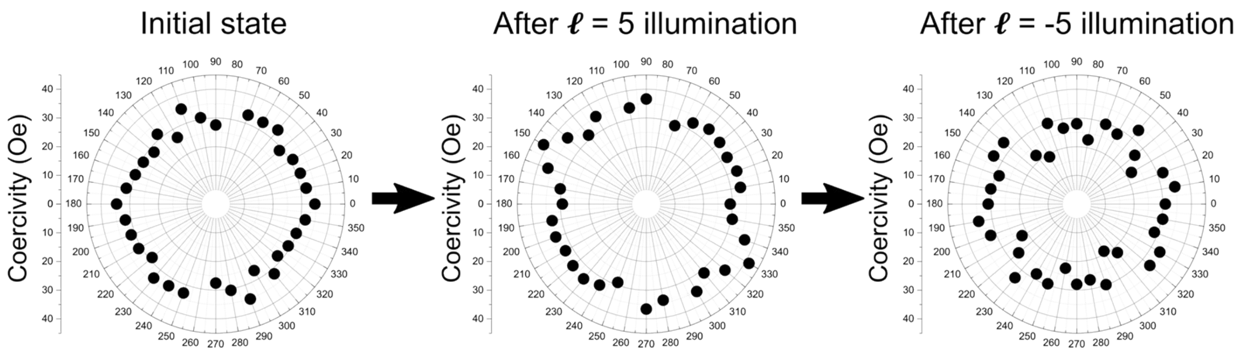


Figure S6. The MA changes after the illumination of the twisted light with positive and negative topological charge $l$ sequentially. From left to right, the initial state of MA of the sample was recorded first and then illuminated by the twisted light of $l = 5$ and $l = -5$, respectively.

**Reversible hysteresis loop transition**

The modified hysteresis loop could revert to the original ferromagnetic loop after waiting for several days. This means the process is reversible. The data are presented in Figure S7. Based on this fact, we believe that the reason of the MA variations is only due to the changes in the alignment of the Co magnetizations. There is no chemical process induced by laser illumination.

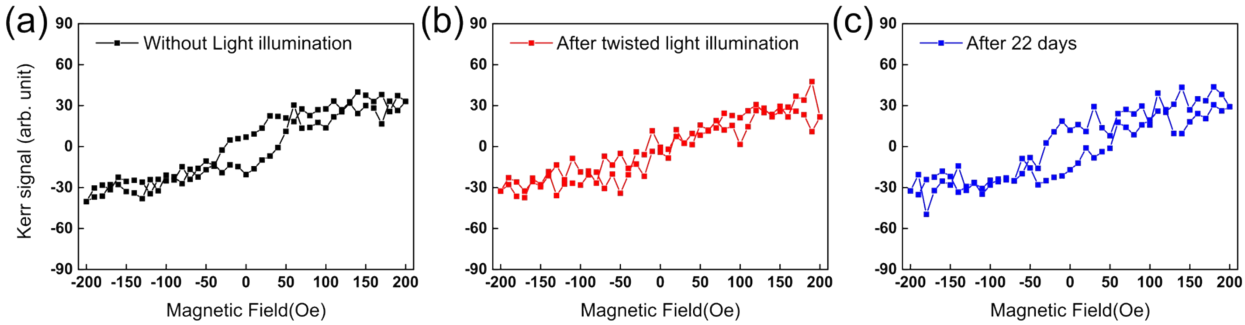


Figure S7: The evolution of the hysteresis loops. The hysteresis loops of the sample (a) before twisted light illumination; (b) after twisted light illumination; and (c) after 22 days, measured again in the same twisted light treated area. The hysteresis seems to recover back to its original state. The sample was kept in a vacuum container during these days.